Fabrication, magnetic properties, and electronic structures of nanoscale zinc-blende MnAs dots (invited)

doi: 10.1063/1.1456396

Fabrication, magnetic properties, and electronic structures of nanoscale zinc-blende MnAs dots (invited)

Kanta Ono[a)]
Department of Applied Chemistry, University of Tokyo, 7-3-1 Hongo, Bunkyo-ku, 113-8656 Tokyo, Japan

Jun Okabayashi
Department of Physics and Department of Complexity Science and Engineering, University of Tokyo, Hongo, Bunkyo-ku, 113-0033 Tokyo, Japan

Masaki Mizuguchi and Masaharu Oshima
Department of Applied Chemistry, University of Tokyo, 7-3-1 Hongo, Bunkyo-ku, 113-8656 Tokyo, Japan

Atsushi Fujimori
Department of Physics and Department of Complexity Science and Engineering, University of Tokyo, Hongo, Bunkyo-ku, 113-0033 Tokyo, Japan

Hiro Akinaga
National Institute of Advanced Industrial Science and Technology (AIST), 1-1-1 Higashi, Tsukuba, Ibaraki 305-8562, Japan

Ferromagnetic nanoscale zinc-blende MnAs dots were successfully fabricated on a sulfur-passivated GaAs (001) surface by molecular-beam epitaxy. Transmission electron microscopy and selected area electron diffraction showed that the crystalline structure was not the same as that of bulk MnAs with NiAs-type hexagonal crystalline structure, but of zinc-blende type. In *in situ* photoemission spectroscopy of the zinc-blende MnAs dots, the Fermi edge was not clearly observed and the Mn $3d$ partial density of states was similar to that of the diluted ferromagnetic semiconductor $Ga_{1-x}Mn_xAs$, which also supports the fabrication of zinc-blende MnAs in the nanoscale. © *2002 American Institute of Physics.* [DOI: 10.1063/1.1456396]

INTRODUCTION

NiAs-type Mn pnictide films grown on GaAs substrates by molecular-beam epitaxy (MBE) have been extensively studied because of their potential as spintronic device applications utilizing ferromagnetic metal–semiconductor hybrid structures. Among them MnAs and MnSb have a higher potential for spintronic devices due to their high Curie temperatures T_c (MnAs: $T_c \sim 320$ K, MnSb: $T_c \sim 600$ K).[1–4] Basic physical properties of MnAs films including the consecutive phase transitions between the NiAs–MnP–NiAs type crystalline structures in the bulk have been investigated.[5] The electronic structure of MBE-grown Mn pnictides films has also been investigated by photoemission spectroscopy including spin-resolved measurements.[6]

Successful combinations of the magnetic properties of the Mn compounds with the semiconducting properties of III–V compound semiconductors has also lead to the creation of a new class of materials called diluted magnetic semiconductors, such as $Ga_{1-x}Mn_xAs$ and $In_{1-x}Mn_xAs$, that have attracted considerable attention in recent years.[7] In particular, the origin of ferromagnetism in these compounds has been extensively studied. It appears that hole carriers in the semiconductors mediate the interaction between the Mn ions that are randomly distributed. The key to the ferromagnetic ordering of the Mn spins is a strong hybridization between the localized Mn $3d$ states and the As $4p$ carriers which results in a strong antiferromagnetic coupling between the spin of the Mn $3d$ electrons and the holes in the As $4p$ valence band. A recent concern in $Ga_{1-x}Mn_xAs$ has been how T_c can be increased. According to the carrier-induced ferromagnetism, to increase T_c, the carrier concentration has to be increased. Ohno *et al.* demonstrated a carrier injection using biased transistor systems to increase the carrier concentration.[8] Photo-induced carriers have also been applied to enhance T_c.[9] However, the Curie temperature of these $Ga_{1-x}Mn_xAs$ has not exceeded 120 K so far, because of the solubility limit of Mn and the carrier self-compensation.[10] To this end, there is a strong demand for the fabrication of the high-concentration limit of $Ga_{1-x}Mn_xAs$, that is MnAs with zinc-blende type crystalline structure, and revealing the physical properties and electronic structures.

Another direction of combining Mn pnictides and GaAs is a fabrication of the Mn pnictides in the nanoscale on GaAs surfaces. Recent development of the MBE growth technique has enabled us to control the geometry of those nanostructures. Akinaga *et al.*[11] and Mizuguchi *et al.*[12] demonstrated that the MnSb nanoscale granular dots grown by MBE on sulfur-passivated GaAs surfaces becomes a promising material for spintronic device applications because of the extremely huge magnetoresistance effect at room temperature. The large surface area of the nanostructures compared with their volume often lead to a relaxation of the lattice in the nanostructures, and enables the fabrication of nanostructure with metastable crystalline structure which is different from the bulk. Recently, the MnAs/GaAs digital magnetic hetero-

[a)]Author to whom correspondence should be addressed; electronic mail: ono@sr.t.u-tokyo.ac.jp

structure was fabricated using MBE by alternately depositing layers of MnAs and GaAs.[13] However, it is reported that only a submonolayer of the MnAs layer can be grown epitaxially and the crystalline structure of the MnAs layer is still unknown.

In this article, we report on the successful fabrication of nanoscale zinc-blende MnAs dots on sulfur-passivated GaAs surfaces grown by MBE and their crystalline structures, magnetic properties, and electronic structures.

EXPERIMENT

The nanoscale MnAs dots were fabricated on sulfur-passivated n^+-GaAs(001) substrates by a conventional solid-source MBE.[14] It is well known that GaAs substrates terminated by VI-element atoms, such as sulfur or selenium, have low surface energy, and thus enable a self-assembled growth of metallic clusters on the semiconductor. To terminate the surface of GaAs substrates by surfur, the substrate was first dipped into an $(NH_4)_2S_x$ solution for 1 h, then rinsed by pure water. By heating the substrates up to 200 °C, the reflection high-energy electron diffraction (RHEED) pattern changes from a halo to a 1×1 streaky pattern. During the growth of MnAs dots at 200 °C, the flux ratio of As/Mn was set at 4–5. The growth of the MnAs dots changed the streaky 1×1 RHEED pattern to a spotty pattern. The surface morphology of the samples was evaluated by *ex situ* atomic-force microscopy (AFM), high-resolution scanning electron microscopy (SEM), high-resolution cross-sectional transmission electron microscopy (TEM), and selected area electron diffraction (SAED). The magnetic properties were measured using a superconducting quantum interference device (SQUID) magnetometer. The MBE system used in this study was connected to the synchrotron radiation photoemission system at BL-1C of the Photon Factory, High-Energy Accelerator Research Organization.[15] Prior to the AFM, SEM, TEM, and SAED measurements, *in situ* photoemission spectroscopy was performed for the MBE-grown MnAs dots and the MBE-grown samples were transferred into the photoemission measurement chamber without breaking the ultrahigh vacuum. For the valence band photoemission measurement, the photon energy was varied from 20 to 130 eV and the emission angle of photoelectrons was set normal to the surface. Photoemission measurements were done at room temperature and the total energy resolution was set at about 100 meV using a hemispherical analyzer (VG Microtec, ARUPS10). For the Mn $2p$ core-level photoemission measurements, Mg $K\alpha$ x-ray radiation was used.

As references, we have grown $Ga_{1-x}Mn_xAs$ and NiAs-type bulk MnAs film on GaAs(001). The growth procedure for the $Ga_{1-x}Mn_xAs$ is as follows.[16] After the removal of a surface oxide layer by heating the substrate to 580 °C, a 15 nm buffer layer of the GaAs was grown at 580 °C with 2×4 reconstruction. After cooling the substrate to 200 °C [$c(4\times4)$ reconstruction], a 10 nm low-temperature (LT) GaAs buffer layer was grown with the 1×1 RHEED pattern. On this LT buffer layer, a 10 nm $Ga_{1-x}Mn_xAs$ layer was grown with the 1×2 surface reconstruction. NiAs-type bulk MnAs films were also grown on the GaAs buffer layer in the same MBE chamber. The substrate temperature and the flux ratio of As/Mn were set at 200 °C and 4–5, respectively, which is equal to the growth condition of nanoscale MnAs dots. In order to compare the Mn $3d$-derived electronic states, *in situ* photoemission measurements have been performed for nanoscale MnAs dots, $Ga_{1-x}Mn_xAs$ film, and NiAs-type bulk MnAs film.

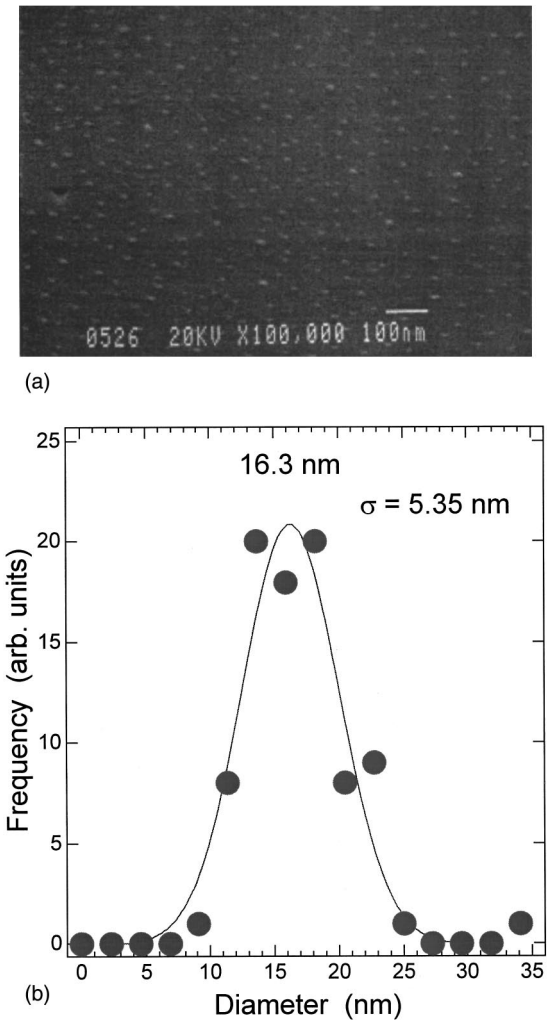

FIG. 1. Surface morphology of the nanoscale MnAs dots grown on a sulfur-passivated GaAs (001) substrate. (a) High-resolution SEM image of the MnAs nanoscale dots. (b) Size distribution of the MnAs nanoscale dots estimated from SEM image.

RESULTS AND DISCUSSION

Figure 1(a) also shows the surface morphology of the nanoscale MnAs dots observed by SEM. The size distribution of the nanoscale MnAs dots is shown in Fig. 1(b). The cross-sectional high-resolution TEM image in Fig. 2 shows that the average height of the dot is 2–5 nm. In the TEM image, clear lattice fringes of the nanoscale MnAs dots as well as the GaAs substrate are observed in both [110] and [1-10] cross sections. The dark contrast at the interface region shows the sulfur layer at the interface. The lattice fringe of the nanoscale MnAs dots is almost the same as that of the GaAs substrate, indicating a formation of zinc-blende crystalline structure of the nanoscale MnAs dots, although a

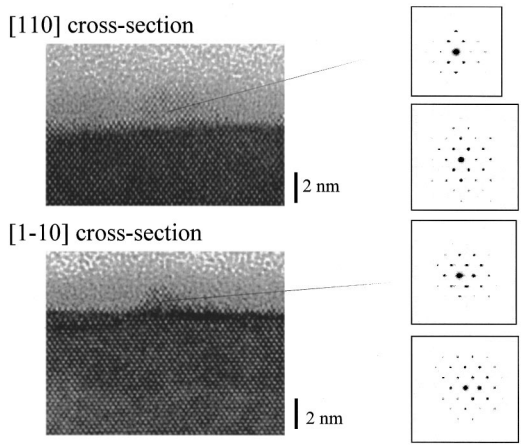

FIG. 2. High-resolution cross-sectional TEM images and SAED patterns of nanoscale MnAs dots and GaAs substrates.

small lattice expansion in the nanoscale MnAs dots is also observed. Without the sulfur passivation, the crystalline structure, observed by the high-resolution TEM of the MnAs film on GaAs was different from that of the GaAs substrate, which suggests that the MnAs film was grown in the hexagonal NiAs-type crystalline structure.[17] It is also noted that in the case of the nanoscale MnSb dots on surfur-passivated GaAs, MnSb dots form a hexagonal crystalline structure.[11] For a more detailed analysis, we have performed SAED measurements for nanoscale MnAs dots and GaAs substrates. The SAED pattern in Fig. 2 clearly shows that the SAED patterns for the nanoscale MnAs dots and GaAs substrate are the same. The TEM and SAED measurements clearly indicate that the crystalline structure of nanoscale MnAs dots is zinc-blende type, not the bulk hexagonal NiAs type.

Here, we discuss in more detail the crystalline structure and the electronic structure of the MnAs dots. From the TEM images and SAED patterns, a lattice expansion parallel to the surface compared with the GaAs substrate is estimated to be 0.7%. In the nanoscale MnAs dots, the lattice is almost completely relaxed, resulting in the small lattice mismatch. The lattice constant of hypothetical zinc-blende MnAs estimated from the extrapolation of the lattice constant of $Ga_{1-x}Mn_xAs$ with $x=1$ is 5.98 Å and considerably large lattice mismatch of 5.8% to GaAs substrate is expected.[16] It is considered that the formation of the zinc-blende structure and small lattice mismatch in nanoscale MnAs dots are derived from the lower surface energy of the sulfur-passivated GaAs surface and lattice relaxation due to the nanoscale dot formation. Note that in the case of the zinc-blende CrAs, the lattice constant of zinc-blende CrAs is almost the same as that of the GaAs substrate and it is possible to grow zinc-blende CrAs films on GaAs substrates.[18]

Magnetic properties of nanoscale zinc-blende MnAs dots are shown in Fig. 3. Figure 3(a) shows the magnetization hysteresis curve taken at 50 K. Clear hysteresis shows that the nanoscale zinc-blende MnAs dots show ferromagnetic ordering. Figure 3(b) shows the temperature dependence of remanent magnetization of the nanoscale zinc-blende MnAs dots. It is estimated that the Curie temperature of the nanoscale zinc-blende MnAs dots is about 280 K.

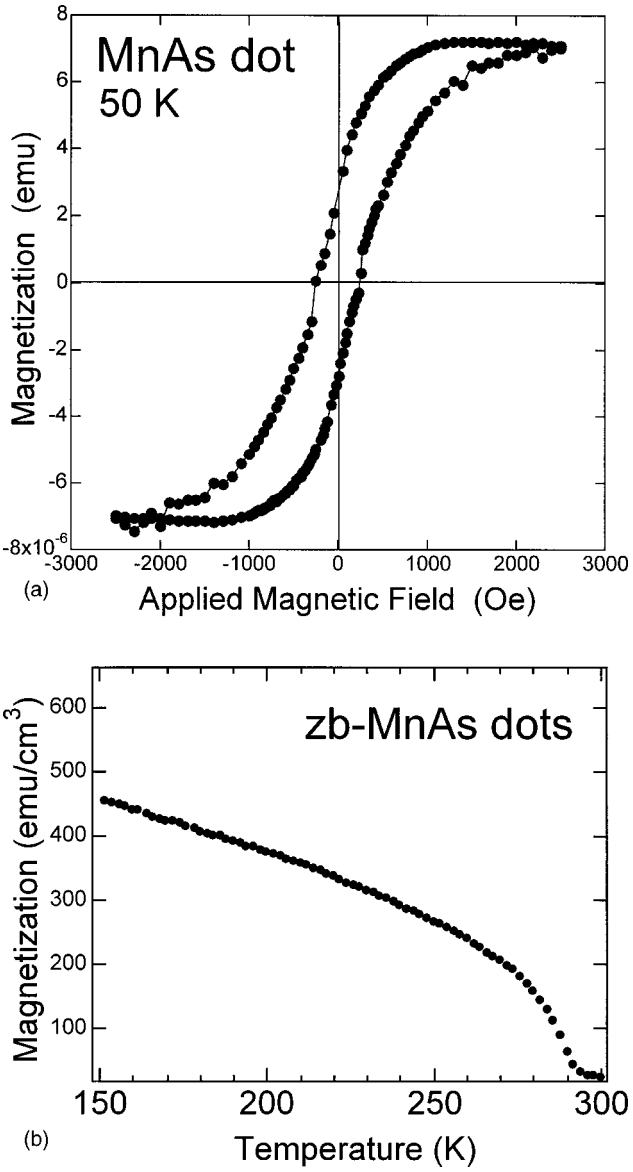

FIG. 3. Magnetic properties of nanoscale zinc-blende MnAs dots. (a) Magnetization hysteresis curve at 50 K. Clear hysteresis shows that the nanoscale zinc-blende MnAs dots show ferromagnetic ordering. (b) Temperature dependence of remanent magnetization of the nanoscale zinc-blende MnAs dots.

The Mn $3d$ partial density of states (PDOS) of the nanoscale MnAs dots shown in Fig. 4(a) was deduced using the $3p-3d$ resonant photoemission technique and is compared with that of $Ga_{1-x}Mn_xAs$ in Fig. 4(b). The Mn $3d$ PDOS has been extracted from the subtraction of the photoemission spectrum taken at 48 eV from that at 50 eV. Figure 4(b) shows valence-band photoemission spectra of the *in situ* prepared $Ga_{1-x}Mn_xAs$. The PDOS of $Ga_{1-x}Mn_xAs$ is similar to that reported previously.[19] The resonant enhancement was observed from E_F to ~10 eV with a prominent peak at ~4 eV binding energy in the photoemission spectra taken at 50 eV. $Ga_{1-x}Mn_xAs$ has the zinc-blende type crystalline structure with the Mn atom tetrahedrally coordinated by As atoms. All the tetrahedrally bonded Mn-based magnetic semiconductors including II–VI compounds reported so far show almost the same electronic structure, that is the main

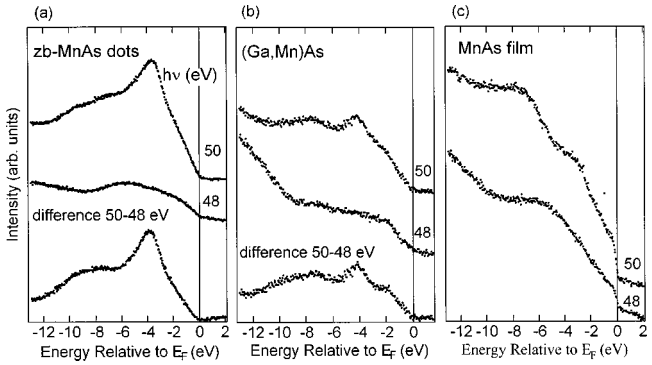

FIG. 4. Valence-band photoemission spectra of *in situ* prepared (a) nanoscale zinc-blende MnAs dots, (b) $Ga_{1-x}Mn_xAs$, and (c) NiAs-type bulk MnAs film. The difference between the on- and off-resonant spectra shows the Mn $3d$ PDOS.

peak located around 4 eV binding energy, a strong satellite structures at deep binding energies around 7–9 eV, and small spectral weight just below E_F.[20] Such an electronic structure has been well understood using the configuration-interaction cluster model and cannot be reproduced within the framework of band-structure calculations,[21] indicating the importance of many-body effects. On the other hand, the photoemission spectra of the MnAs films in Fig. 4(c) do not show a 4 eV peak nor a satellite but show a clear Fermi-edge characteristic of a metallic sample. Strong Auger structure from the As $3d$ core level also overlaps the valence-band region as reported in Ref. 6.

The photoemission spectra of the nanoscale MnAs dots prepared *in situ* show almost the same electronic structure as the $Ga_{1-x}Mn_xAs$, quite different from the photoemission spectra of the MnAs films. From the viewpoint of photoemission spectroscopy, the electronic structure of the nanoscale MnAs dots is similar to $Ga_{1-x}Mn_xAs$. This means that Mn $3d$ electrons are essentially localized in the nanoscale MnAs dots, as opposed to the case in the MnAs bulk where Mn $3d$ electrons are itinerant. The nanoscale MnAs dots were found to form in the zinc-blende crystalline structure as shown in the TEM image, which is consistent with the photoemission results. It is concluded that the Mn $3d$ electrons in the nanoscale zinc-blende MnAs dots are localized due to the many-body effect.

The band-structure calculation has been performed for the hypothetical zinc-blende MnAs.[22,23] The result shows a high DOS at E_F unlike the photoemission results probably due to the many-body effect, but only the Mn $3d$ main peak at 4 eV binding energy in the MnAs nanoscale dots can be interpreted within the band-structure calculation.

Figure 5 shows the Mn $2p$ core-level photoemission spectra for *in situ* prepared nanoscale zinc-blende MnAs dots, $Ga_{1-x}Mn_xAs$, and NiAs-type bulk MnAs film. The satellite structure, which is originated from the many-body effect, is observed in nanoscale zinc-blende MnAs dots and $Ga_{1-x}Mn_xAs$. It also indicates the electron localization in the nanoscale zinc-blende MnAs dots.

The failure of the application of the band-structure calculation to the description of the electronic structure and electron localization due to the many-body effect in the

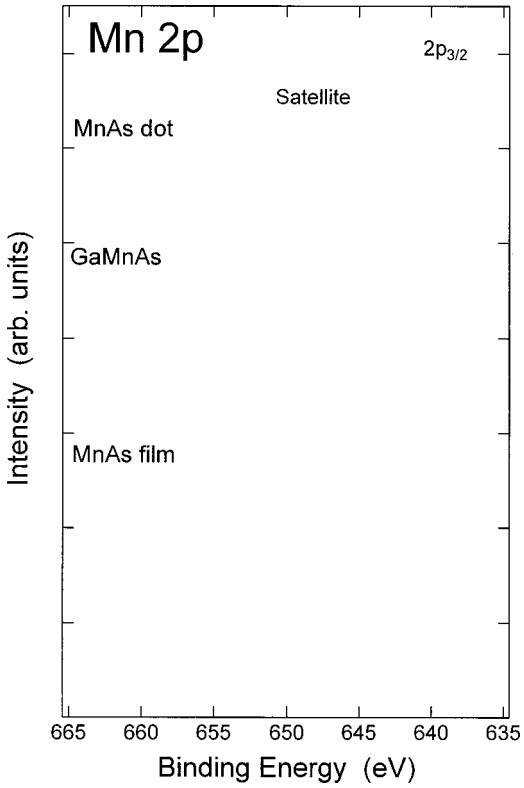

FIG. 5. Mn $2p$ core-level photoemission spectra of *in situ* prepared nanoscale zinc-blende MnAs dots, $Ga_{1-x}Mn_xAs$, and NiAs-type bulk MnAs film.

nanoscale zinc-blende MnAs dots opens a category of nanoscale materials with correlated-electron systems. An extensive investigation of the nanoscale zinc-blende MnAs dots for the basic physical properties as well as the spintronic device application is strongly needed.

CONCLUSION

In conclusion, MnAs nanoscale dots were successfully fabricated on the sulfur-passivated GaAs(001) substrates and were characterized by SEM, TEM, SAED, SQUID, and *in situ* photoemission measurements. The existence of the ferromagnetic zinc-blende MnAs has been proven experimentally. The electronic structure of zinc-blende MnAs evaluated by photoemission measurements is similar to that of $Ga_{1-x}Mn_xAs$. It is found that the Mn $3d$ electrons in the nanoscale zinc-blende MnAs dots are localized due to the many-body effect. It is reasonably considered that the zinc-blende MnAs is the high-concentration limit of $Ga_{1-x}Mn_xAs$.

ACKNOWLEDGMENTS

This work was done under Project No. 97S1-002 at Institute of Material Structure Science at KEK, and partly supported by the New Energy and Industrial Technology Development (NEDO). This work was partly supported by a Grant-in-Aid for Scientific Research (Grant No. B2-13554012) from Ministry of Education, Culture, Sports, Science, and Technology. The authors would like to thank Professor M. Shirai for the helpful discussion.

[1] J. De Boeck, R. Oesterholt, A. Van Esch, H. Bender, C. Bruynseraede, C. Van Hoof, and G. Borghs, Appl. Phys. Lett. **68**, 2744 (1996).
[2] H. Akinaga, S. Miyanishi, K. Tanaka, W. Van Roy, and K. Onodera, Appl. Phys. Lett. **76**, 97 (2000).
[3] S. H. Chun, S. J. Potashnik, K. C. Ku, J. J. Berry, P. Schiffer, and N. Samarth, Appl. Phys. Lett. **78**, 2530 (2001).
[4] H. Shimizu, M. Miyamura, and M. Tanaka, Appl. Phys. Lett. **78**, 1523 (2001).
[5] K. Adachi, J. Phys. Soc. Jpn. **16**, 2187 (1961).
[6] K. Shimada, O. Rader, A. Fujimori, A. Kimura, N. Kamakura, A. Kakizaki, K. Ono, M. Tanaka, and M. Shirai, J. Electron Spectrosc. Relat. Phenom. **88–91**, 207 (1998).
[7] H. Ohno, Science **281**, 951 (1998) and references therein.
[8] H. Ohno, D. Chiba, F. Matsukura, T. Omiya, E. Abe, T. Dietl, Y. Ohno, and Y. Ohtani, Nature (London) **408**, 944 (2000).
[9] S. Koshihara, A. Oiwa, M. Hirasawa, S. Katsumoto, Y. Iye, C. Urano, H. Takagi, and H. Munekata, Phys. Rev. Lett. **78**, 4617 (1997).
[10] T. Dietl, H. Ohno, F. Matsukura, J. Cibert, and D. Ferrand, Science **287**, 1019 (2000).
[11] H. Akinaga, M. Mizuguchi, K. Ono, and M. Oshima, Appl. Phys. Lett. **76**, 357 (2000).
[12] M. Mizuguchi, H. Akinaga, K. Ono, and M. Oshima, Appl. Phys. Lett. **76**, 1743 (2000).
[13] R. K. Kawakami, E. Johnston-Halperin, L. F. Chen, M. Hanson, N. Guebels, J. S. Speck, A. C. Gossard, and D. D. Awschalom, Appl. Phys. Lett. **77**, 2379 (2000).
[14] M. Oshima *et al.*, Jpn. J. Appl. Phys., Part 1 **38-1**, 373 (1999).
[15] K. Ono *et al.*, Nucl. Instrum Methods Phys. Res. A (in press).
[16] H. Ohno, A. Shen, F. Matsukura, A. Oiwa, A. Endo, S. Katsumoto, and Y. Iye, Appl. Phys. Lett. **69**, 363 (1996).
[17] A. Trampert, F. Schippan, L. Daweritz, and K. H. Ploog, Appl. Phys. Lett. **78**, 2461 (2001).
[18] H. Akinaga, T. Manago, and M. Shirai, Jpn. J. Appl. Phys., Part 1 **39**, 1118 (2000).
[19] J. Okabayashi, A. Kimura, T. Mizokawa, A. Fujimori, T. Hayashi, and M. Tanaka, Phys. Rev. B **59**, 2486 (1999).
[20] T. Mizokawa and A. Fujimori, Phys. Rev. B **48**, 14150 (1993).
[21] J. H. Park, S. K. Kwon, and B. I. Min, Physica B **281–282**, 703 (2000).
[22] M. Shirai, T. Ogawa, I. Kitagawa, and N. Suzuki, J. Magn. Magn. Mater. **177–181**, 1383 (1998).
[23] S. Sanvito and N. A. Hill, Phys. Rev. B **62**, 15553 (2000).